SUPPORTING INFORMATION

An Allosteric Inhibitor Scaffold Targeting the PIF-Pocket of Atypical Protein Kinase C Isoforms

Jose M. Arencibia, Wolfgang Fröhner, Magdalena Krupa, Daniel Pastor-Flores, Piotr Merker, Thomas Oellerich, Sonja Neimanis, Christian Schmithals, Verena Köberle, Evelyn Süß, Stefan Zeuzem, Holger Stark, Albrecht Piiper, Dalibor Odadzic, Jörg O. Schulze, Ricardo M. Biondi*

Supplementary Methods

Structural studies

The PDK1-PKCι chimera was crystallized by hanging drop vapor diffusion at 20 °C. 1.5 µl of protein (23 mg/ml) was added to 1.5 µl of reservoir solution (1.25 M sodium citrate, 100 mM HEPES pH 7.5 and 10mM DTT) and 0.3 µl of 1 M ammonium sulfate. Crystals grew to a size of 300 µm x 300 µm x 80 µm within two to three weeks. For the PS267-bound structure, crystals were soaked for 18 h in reservoir solution containing 1.5 mM PS267. X-ray diffraction data were collected on BL14.1 operated by the Helmholtz-Zentrum Berlin (HZB) at the BESSY II electron storage ring. Data were processed and scaled using the XDS program package (*1*). The structure of dmPDK1 50-359 (PDB code 3HRC) (*2*) served as model in molecular replacement using Phaser (*3*). PHENIX was used for refinement, including TLS protocols (*4*). Coot was used for manual model building and structural analysis (*5*). Molecular graphic figures were prepared using PyMOL(*6*).

Yeast-based chemical-genetic assay

The assay was set-up using an *S. cerevisiae* strain (SDP10) that is deleted in erg6, favoring the permeability of compounds into yeasts (*7*). SDP10 colonies containing pRS316 or pRS316-*BCK1-20* were grown overnight at 30°C in selective growth medium. The cells were then washed and gently resuspended in 50 mM Tris, 10 mM EDTA buffer supplemented with 50% PEG. Compounds (200 µM final concentration) or DMSO (control) were then added to the cells and incubated for 30 min at 30°C. Aliquots of the cells where then incubated in a water bath at 42°C for 15 min in the presence or absence of the chemical compounds. The samples were then left on ice for 2 min, washed and resuspended in cold PBS. Finally, the cells were incubated in

the liquid selective growth medium and the OD630 nm was measured after 21 hr. Alternatively, 10-fold serial dilutions of the cells were spotted in selective agar dishes and grown for 36 hr.

Cell proliferation assay

Lung cancer cell lines A549, A427 and colon cancer cell line HCT116 were obtained from DMSZ. DU145 prostate cancer cell line and PNT1A immortalized normal prostate epithelial cell line were obtained from Sigma-Aldrich. All cells were routinely maintained in RPMI-1640 (Gibco) supplemented with 10% heat-inactivated FBS (Sigma-Aldrich) and kept at 37°C in a humidified atmosphere containing 5% CO_2. Anchorage-dependent cell proliferation assays were performed using the MTT method. Briefly, cells were seeded in 96 well plates at a density of 10^4 cells/well in 100 µl medium and allowed to attach overnight. Compounds were serially diluted using culture medium and 100 µl of 2X final concentration was added into the wells. After 48 h incubation, 5 mg/ml solution of MTT in PBS was added to the wells and further incubated for 2hr. After removing the medium, MTT-formazan salts were dissolved using DMSO and absorbance read in a multiplate reader at 590 nm. Pharmacological interaction between PS432 and PI3-kinase or proteasome inhibitors (Selleckchem) was assessed by CompuSyn software using the Chou and Talalay combination index (CI) method (*8*). CI <1, =1, and >1 indicate synergy, additive effect, and antagonism, respectively.

Soft-agar colony formation assay

Anchorage-independent cell growth was performed in 96 well plates as described (*9*). Briefly, $5x10^3$ cells/well were seeded in a 0.3% SeaPlaque agarose (Lonza) solution in complete medium over a 0.6% SeaPlaque agarose layer in complete medium. Twenty four hours later different concentrations of compounds were added in complete medium and the cells were incubated for additional 7 days. Cell proliferation was assessed using alamarBlue (AbDSerotec) and fluorescence intensity was measured with an EnVision Multilabel Plate Reader (Perkin Elmer) using excitation filter BODIPY TMR FP 531 and emission filter Rhodamine 590.

Cell cycle analysis by flow cytometry

A549 cells were seeded in 100 mm dishes at a density of $1.5x10^6$ cells per dish and allowed to attach overnight. The media was replaced the following day with medium containing DMSO as control or PS432 at different concentrations and incubated for the indicated times. Cells were then recovered by trypsinization and after a wash in cold PBS, fixed with 70% ethanol at 4°C overnight. Fixed cells were washed twice with PBS and then stained with a solution containing 0.2 mg/ml RNase A (Sigma-Aldrich) and 0.1 mg/ml propidiumiodide (Sigma-Aldrich) in PBS for 30 minutes at 37°C. DNA content was measured using a FACSCalibur flow cytometer (Becton Dickinson) and data analyzed using FlowJo software (v7.1.3. Tree Star Inc.).

Immunoblotting

A549, DU145 or HCT116 cells were seeded 1 day before treatment with medium containing PS432 at different concentrations or DMSO as control. Following treatment, proteins were extracted, electrophoresed on NuPAGE10% Bis-Tris gels (Invitrogen) and transferred into nitrocellulose membranes. For the analysis of the expression of cell cycle-related proteins, A549 were enriched in G1 phase by serum starvation for 24 h and then released into medium containing either 50 μM PS432 or DMSO as control. Cells were harvested at the indicated times and analyzed by immunoblotting. Primary antibodies used in this study include the following:anti-CDK7/CAK and anti-β-actin (Sigma-Aldrich); anti-phospho-CDK7 (T170) (ABCAM); anti-phospho-CDK2 (T160), anti-phospho-S6 (S235/236), anti-phospho-NDRG1 (Thr346) and anti-PARP (Cell Signaling). The bound antibodies were detected by using the horseradish peroxidase-conjugated anti-rabbit or anti-mouse IgG (Sigma-Aldrich) and Luminata Forte Western HRP substrate (Millipore). Chemiluminescence was detected using the LAS-4000 imaging system (Fuji) and analyzed using the MultiGauge V3.2 software.

Microarray analysis of gene expression

A549 cells were seeded in 100 mm dishes at a density of $1.5x10^6$ cells per culture dish and allowed to attach overnight. Next day medium was replaced with medium containing 25 μM PS432 or DMSO as control and further incubated for different times. Medium and cells were recovered together and after washing with PBS, RNA was extracted using RNeasy kit (QIAGEN) following the manufacturer's instructions. Quality and concentration of RNA was analyzed using a 2100 Bioanalyzer (Agilent) and then hybridized to Agilent Human 8x60K Microarray (Atlas Biolabs GmbH). Raw data was analyzed using BRB-array tools (v4.2.1) developed by Dr. Richard Simon and BRB-ArrayTools Development Team (*10*) and GO term analysis of differentially expressed genes was performed using gprofiler and GSEA web based tools (*11, 12*). The microarray data have been deposited in the Gene Expression Omnibus database (GSE63593)

SILAC labelling, biochemical processing and mass spectrometry

A549 cells were grown in SILAC (stable isotope labeling of cell cultures by amino acids) RPMI medium containing dialyzed FBS (Sigma), Penicillin/Streptomycin (Invitrogen) and the respective SILAC amino acids (all Cambridge Isotopes) until we observed more than 98% SILAC labeling efficacy. Three differentially labeled SILAC batches were generated. Therefore we used for the light cultures (L) $^{12}C_6$,$^{14}N_2$-Lys and $^{12}C_6$,$^{14}N_4$-Arg (lysine +0/ arginine +0), for the intermediate cultures (I) $^{2}D_4$,$^{12}C_6$,$^{14}N_2$-Lys and $^{13}C_6$,$^{14}N_4$-Arg (lysine +4/ arginine+6) and for the heavy cultures (H) $^{13}C_6$,$^{15}N_2$-Lys and $^{13}C_6$,$^{15}N_4$-Arg (lysine +8/ arginine +10). In one set of experiments we

treated the differentially labeled batches for 0 (L), 4 (I) and 8 (H) hours with 25 µM of PS432 or the corresponding DMSO concentrations as a control. In the other set they were treated for 0 (L), 12 (I) and 24 (H) hours with 25 µM of PS432 or the corresponding DMSO concentrations. Upon treatment, 10^6 cells per condition were subjected to lysis as described (*13*) and the resulting proteins of the differentially labeled cell batches were afterwards pooled in equimolar amounts. The proteins were subsequently separated by 1D gel electrophoresis using NuPAGE Bis-Tris Precast Gels (Invitrogen). After commassie-brilliant blue staining the resulting protein lanes were cut into 23 slices. The subsequent tryptic digest and the mass spectrometric protein analysis was performed as described (*13*). Raw data sets were analyzed by using the MaxQuant software (Version 1.0.12.31) in combination with Mascot search engine for peptide and protein identifications (Version 2.2.04, Matrix Science). *Homo sapiens* sequence database IPI human (Version 3.81) was used in forward and reverse versions. GO term analysis of differentially expressed proteins was performed as described above.

Table S1.Crystal structure data collection and refinement statistics

Data collection	
Unit cell dimensions *a*, *b*, *c* (Å)	149.1, 44.5, 47.8
Space group	C2
Wavelength	0.91841
Number of unique reflections	57639
Resolution range (Å)	47-1.41 (1.51-1.41)
Completeness of data (%)	97.1 (96.2)
Redundancy	2.5 (2.6)
R_{sym} (%)	4.7 (48.0)
$<I/\sigma(I)>$	13.0 (2.0)
Refinement	
Maximal resolution (Å)	1.41 (1.43-1.41)
No. of atoms: protein, ligands,	2383, 53, 347
Monomers per asymmetric unit	1
R-factor (%)	13.9 (24.4)
R_{free} (%)	17.4 (28.0)
Wilson *B*-factor (Å^2)	20.1
R.m.s.d. bond length (Å)	0.016
R.m.s.d. bond angles (°)	1.6
Ramachandran plot [a]	96.8/2.8/0.4

[a] Coot (*14*): preferred regions/allowed regions/outliers.

The values in parentheses refer to the shell of highest resolution.

Table S2. Effect of PS432 on the activity of atypical PKCs and representative members of other PKC subfamilies

Protein kinase	Remaining activity (%)
PKCι-FL	25
PKCι-CD	18
PKCζ-FL	28
PKCζ-CD	16
PKCα	193
PKCβII	125
PKCθ	120
PKCδ	147

FL, full length; CD, Catalytic domain.

The selectivity of PS432 was evaluated using different isoforms from the classical (PKCα and PKCβII), novel (PKCθ and PKCδ) and atypical (PKCι and PKCζ) subfamilies of PKC proteins. Results show the percentage of remaining activity after treatment with 25 μM PS432. The kinase activities were measured as previously described (*15*). At present we cannot discard that the measured increased in activity of PKCα may be due to interaction with the PIF-pocket site on this kinase.

Table S3. Effect of PS432 on the activity of representative members of the AGC group of protein kinases

Protein kinase	PS432 (μM)		
	0.5	10	200
PDK1	92	85	106
PKB/Akt (146-464)	110	124	107
RSK1 (1-374)	107	107	118
MSK1 (1-370)	116	92	101
SGK ΔN [422D]	99	48	4
S6K T2 [412E]	96	68	22
Aurora A	125	120	95

Results show the percentage of remaining activity after incubation with the indicated concentrations of PS432. PDK1 has the PIF-pocket exposed and can be activated by HM polypeptides and small molecules that bind to the PIF-pocket (*2*). The employed constructs of AGC kinases RSK1 and MSK1 comprise only the N-terminal protein kinase catalytic domain and lack the HM; RSK1, MSK1, SGK1 and PKBβ/Akt2 constructs used are suitable for activation by HM polypeptides, as previously described (*16*). The results indicate that a series of related kinases that have a functional regulatory PIF-pocket are not inhibited by PS432. PS432 inhibited *in vitro* the activity of S6K1-T2-[412E], a kinase construct that lacks the last 104 aminoacids and the HM phosphorylation site is replaced by Glu. Similarly, PS432 inhibited SGKΔN [422D] a truncated form of SGK lacking 60 residues at the N-terminus which has Asp replacing the phosphorylation site of the HM. However, PS432 did not inhibit the phosphorylation of S6K and SGK downstream targets in cells (SI Figure2).

SI Figure 1

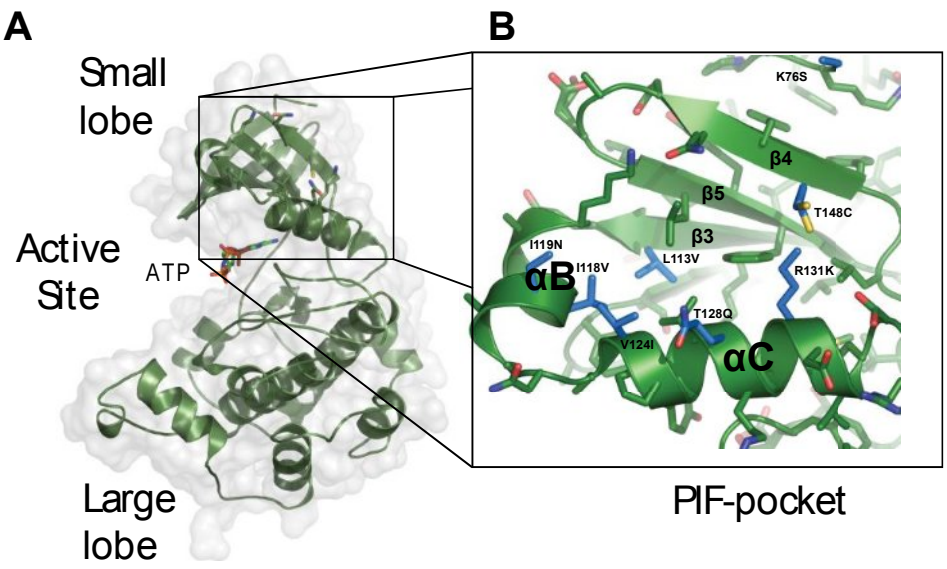

The PIF-pocket, a regulatory site on the small lobe of aPKC and other AGC protein kinases. (A) Ribbon representation of the conserved catalytic domain of protein kinases, comprising a small lobe, a large lobe and the active site, with the ATP-binding site located in between the two lobes. The PIF-pocket is located in the small lobe of the kinase domain (*17-19*). Here, the PIF-pocket is shown unoccupied. A close-up of the PIF-pocket is shown in (B). In active AGC kinases, the PIF-pocket site is occupied by a hydrophobic motif that is located C-terminal to the catalytic core. AGC kinases, like PKB/Akt, S6K, SGK, RSK, MSK, cPKCs require a phosphorylation at the HM for the activation. The activation process mediated by the phosphorylated hydrophobic motif is due to an allosteric communication between the PIF-pocket and the ATP-binding site (*2, 20*). aPKCs, as well as PRKs, posses an acidic residue instead of a phosphorylation site at the HM. The allosteric effects between the the PIF-pocket and the ATP-binding site have been mostly investigated in the protein kinase PDK1 (*21*); The allosteric effect between the PIF-pocket and the substrate/pseudosubstrate-binding site has also been described in aPKCs and PRK2 (*22-25*). In these cases, the binding of the hydrophobic motif to the PIF-pocket displaces the pseudosubstrate binding. In aPKCs, the helix αC can be very mobile and is strongly stabilized by the N-terminal region. Mutagenesis and Hydrogen/Deuterium exchange experiments indicate that the C1 domain is responsible for the inhibition of aPKCs stabilizing the polypeptide comprising the αC helix (*25*). Thus, there is experimental evidence indicating that the PIF-pocket site of aPKCs plays a central role in the physiological regulation of the activity of the kinase, both for the inhibition and for the activation of the kinase.

SI Figure 2

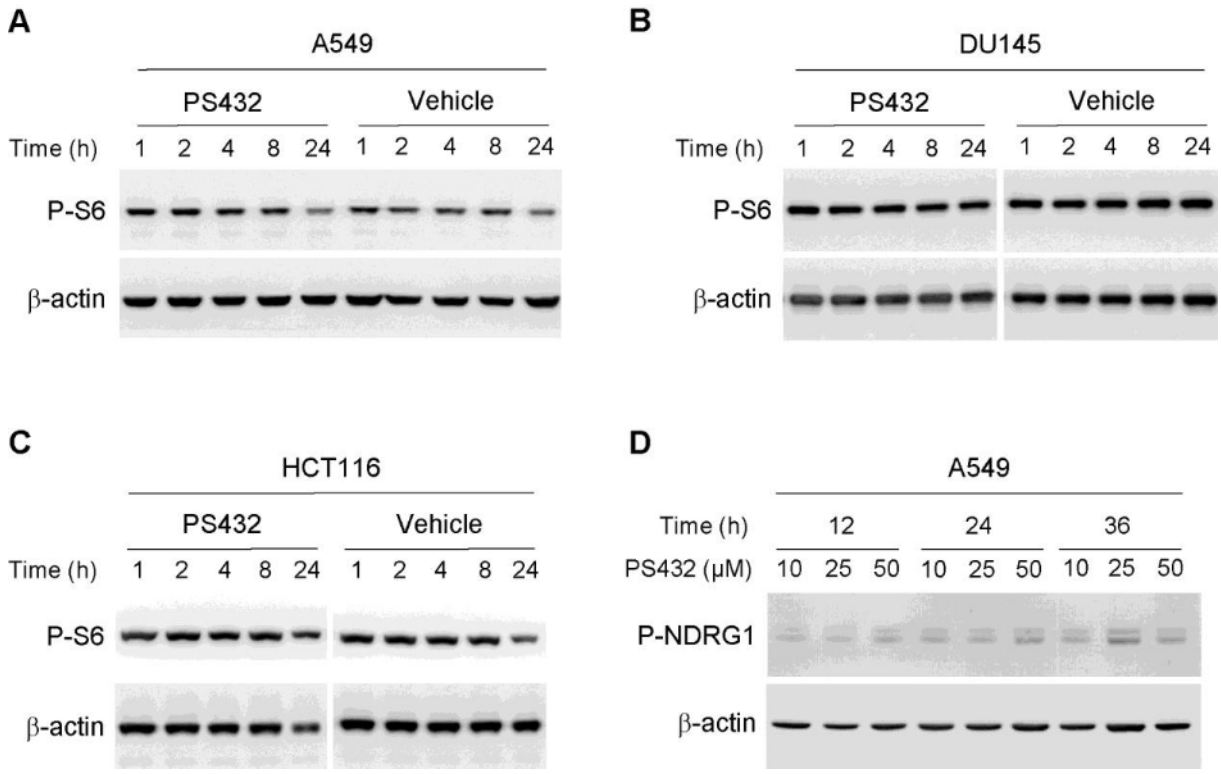

PS432 does not inhibit S6K or SGK signaling. The effect on the phosphorylation of S6 protein, a target of S6K was determined in A549 (A), DU145 (B) and HCT116 (C) cells. The cells were treated with either 25 μM PS432 or vehicle (DMSO) for the indicated time periods. Whole cell lysates were obtained and subjected to western-blot analysis using anti-phospho-S6 (S235/236) antibody. (D) The effects of PS432 on the phosphorylation of SGK substrate NDRG1 in A549 cells. The cell were treated with PS432 at the indicated concentrations for 12, 24 and 36 hours. Protein extracts were prepared and analyzed by western-blotting using anti-phospho-NDRG1 (Thr346) antibody.β-actin is shown as loading control.

SI Figure 3

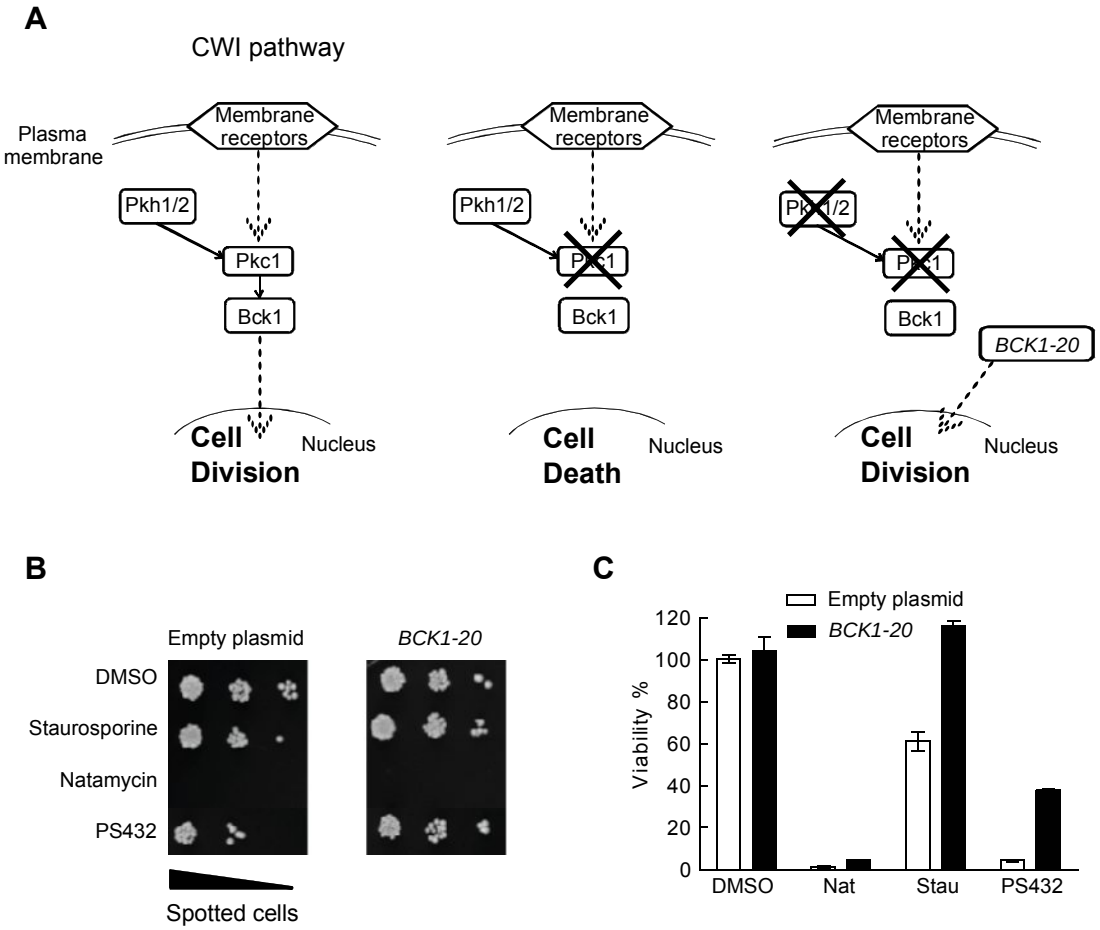

Yeast-based chemical-genetic assay. (A) The yeast Cell Wall Integrity (CWI) signaling pathway is composed of Pkh1/2, Pkc1 and Bck1 protein kinases homologous to human PDK1, PKC and MEKK, respectively. (B) The inhibitory effect of PS432 on the growth of yeasts on solid medium was reverted by the overexpression of constitutively active *BCK1-20.* Yeast cells transformed either with empty or *BCK1-20*-containing vector were subjected to the indicated treatments and 1:10 dilutions of the cells were spotted onto YPD agar plates. (C) The inhibitory effect of PS432 on the growth of yeasts in suspension cultures was bypassed by the overexpression of *BCK1-20.* The culture density of each sample was determined by measuring the absorbance at 630 nm. The effect of natamycin, a polyene antibiotic with broad antifungal spectrum, was not reverted by overexpression of *BCK1-20*.

SI Figure 4

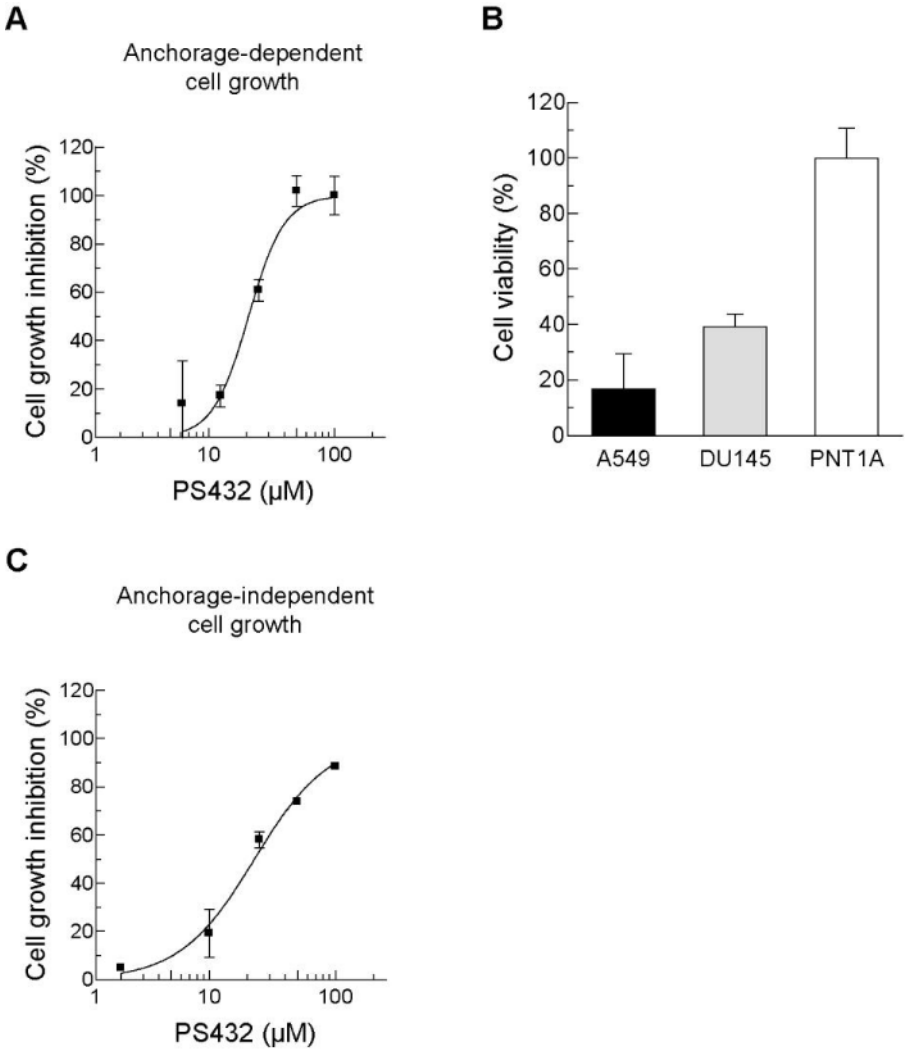

The effect of PS432 on cell proliferation.

(A) Anchorage-dependent cell proliferation of DU145 prostate cancer cells measured by the MTT method after 48 h treatment with various concentrations of PS432. (B) Viability of A549, DU145 and normal prostate epithelial PNT1A cells after 48 h treatment with 25 μM PS432. Bars represent percentage of viable cells assessed using the MTT assay. Error bars represent SD. (C) Anchorage-independent proliferation of DU145 cells using a 1-week 96-well soft agar colony formation assay.

SI Figure 5

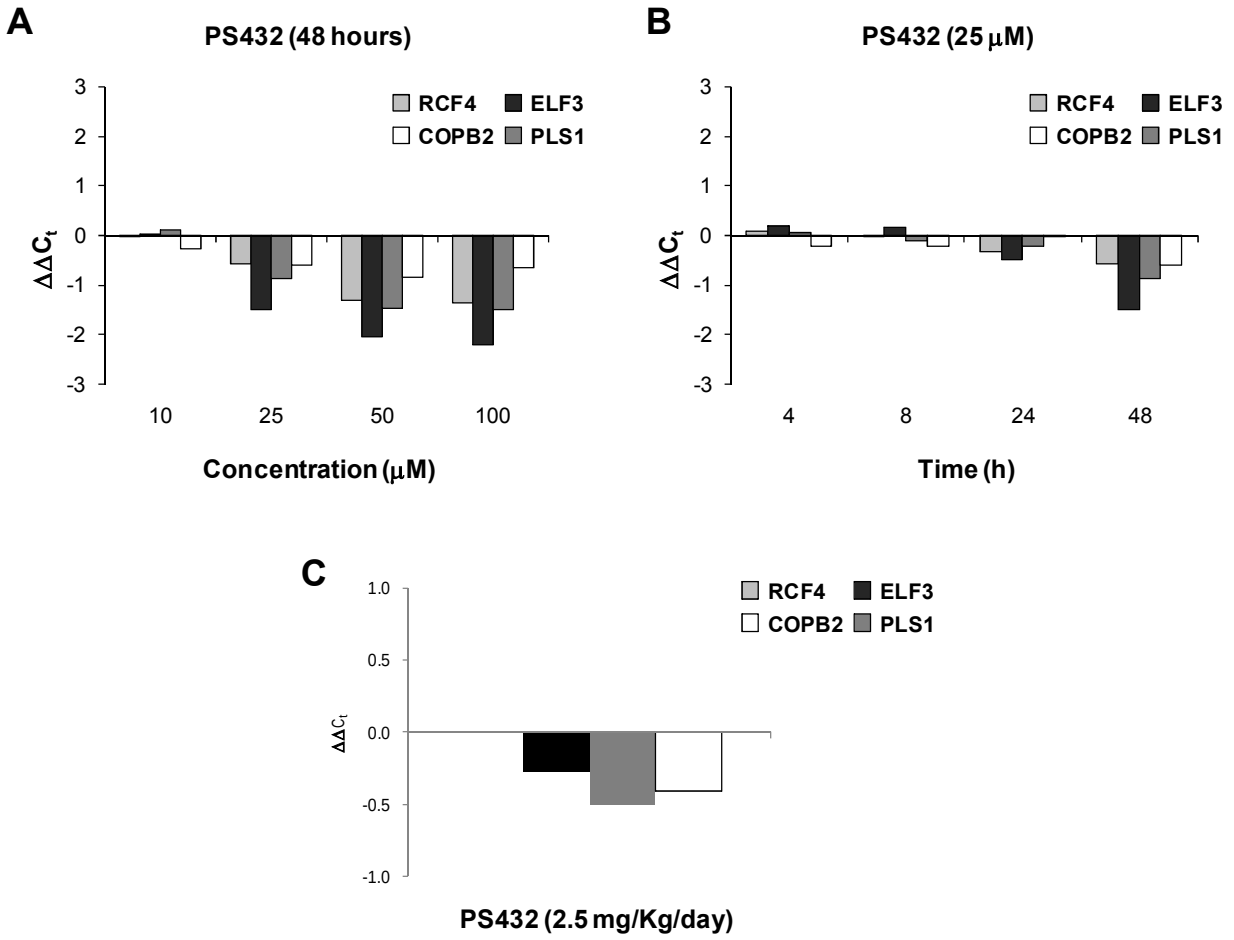

PS432 inhibits the expression of genes regulated by PKCι. PKCι regulates the expression of RCF4, ELF3, PLS1 and COPB2 genes in lung cancer cell lines, and knock-down of PKCι leads to inhibition of their expression (*26*). Treatment of A549 cells with (A) different concentrations of PS432, or (B) with 25 μM PS432 for different times, induced the decrease in mRNA expression levels of target genes. (C) Treatment of mice bearing A549 tumors with PS432 a daily dose of 2.5 mg/Kg caused downregulation of the mRNA levels for ELF3, PLS1 and COPB2 genes.

SI Figure 6

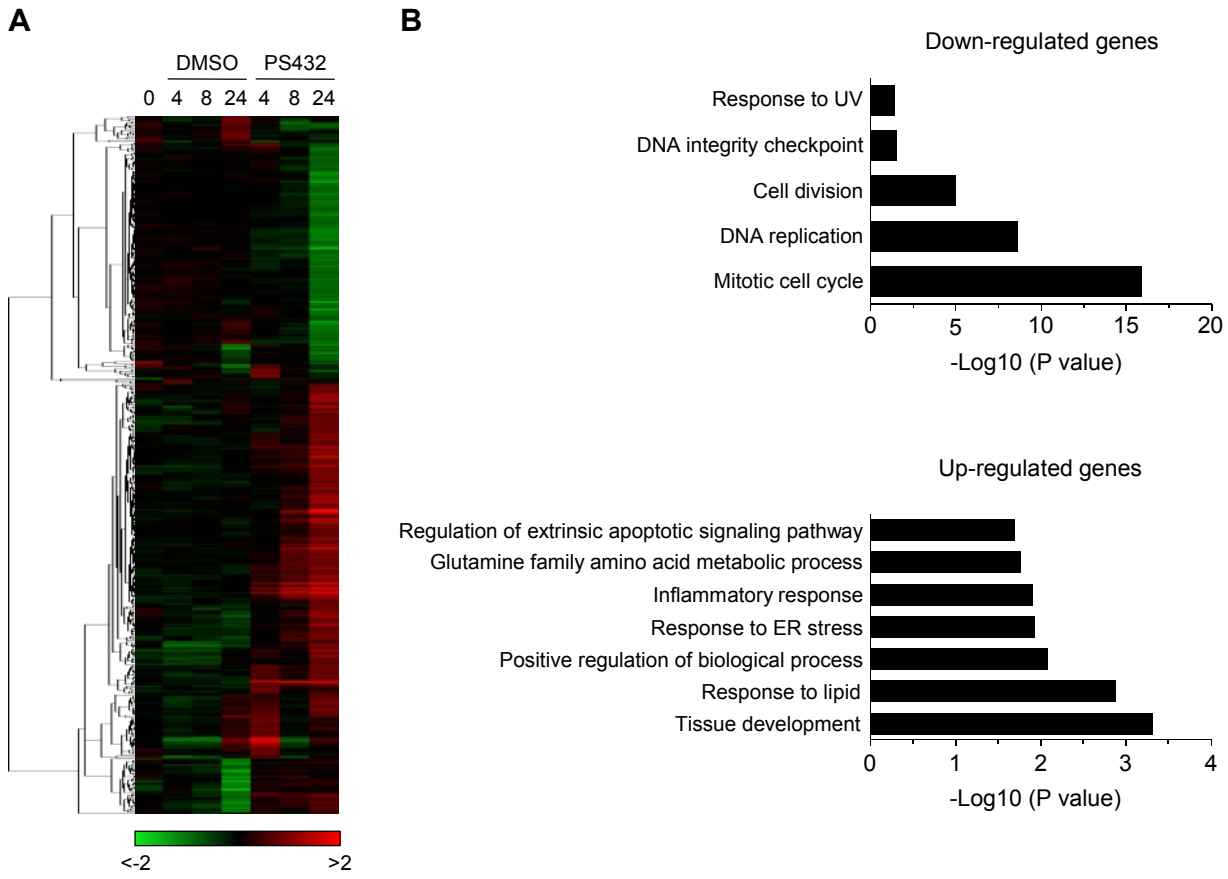

Effect of PS432 on gene expression. (A) Differentially expressed genes were subjected to hierarchical cluster analysis using complete linkage by Pearson's correlation to classify genes according to similar patterns of expression after treatment with 25 μM PS432. Each line in the heat map represents a gene and each column the indicated time of treatment in hours. Dendrogram on the left of the heat map represents correlation distance for each gene. Color bar under the heat map represents the level of expression. (B) Gene ontology terms of biological processes of genes that were differentially expressed in A549 lung cancer cells after treatment with PS432.

SI Figure 7

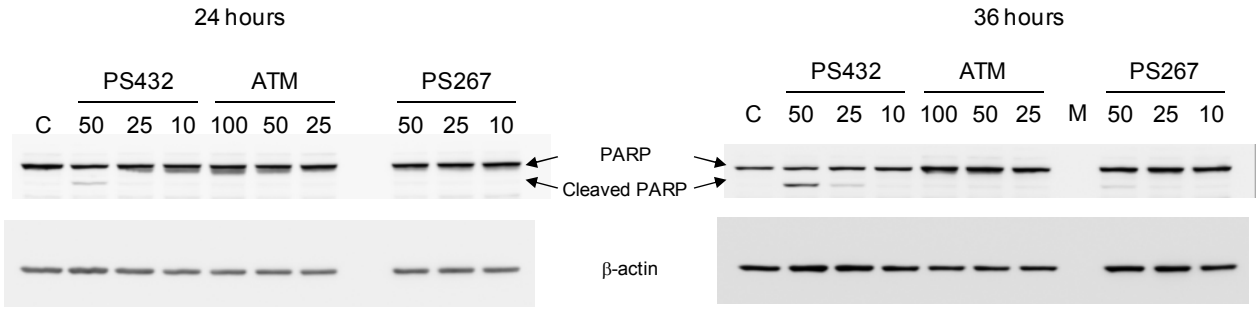

Time- and concentration- dependent modulation of PARP cleavage and pCDK7 by PS432. There is an increase in the cleaved form of PARP that is time and concentration dependent when the cells were treated with the allosteric inhibitors PS432 and PS267. The PKCι inhibitor ATM has no effect on PARP cleavage at the concentrations tested. For this study, A549 cells growing asynchronously were treated with aPKC inhibitors at different concentrations for the indicated times. After treatment, cells were lysed and 50 μg protein from the cleared extract were separated by electrophoresis and transferred into nitrocellulose membrane. After blocking in 5% non-fat milk in TBST buffer, blots were incubated overnight at 4°C with the indicated primary antibodies and developed as described in supplementary information. The concentration of each compound (μM) is indicated above each line. C: control (DMSO treated); M: Molecular weight marker.

SI Figure 8

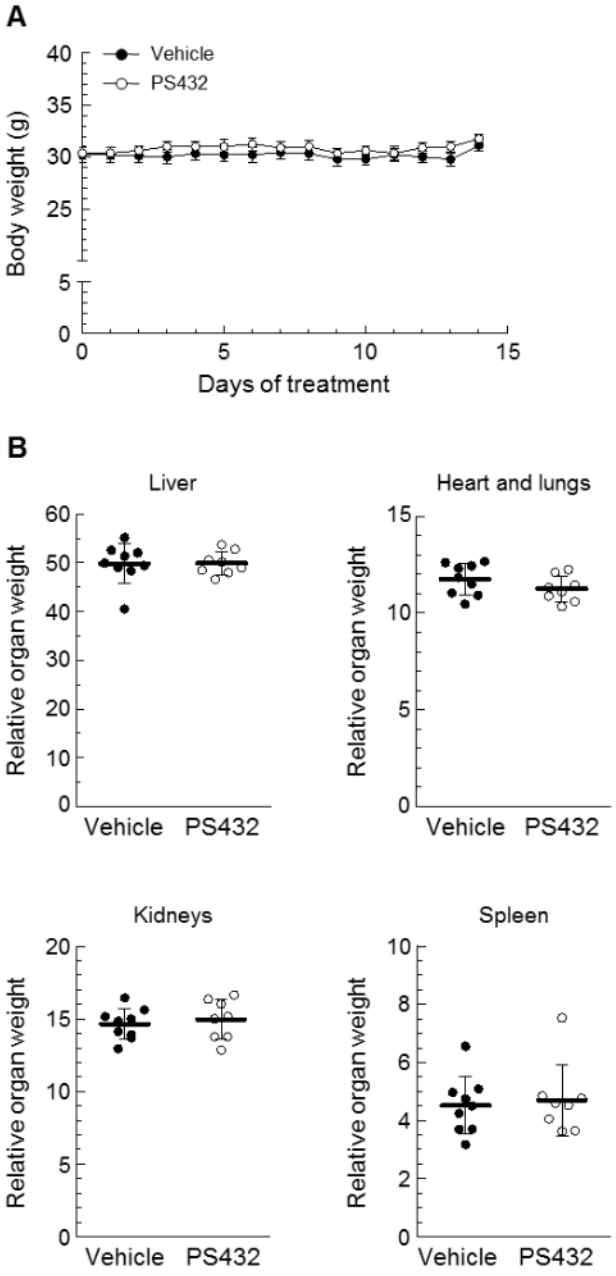

The treatment of A549 xenograft-bearing mice with PS432 does not alter substantially neither body or major organs weight. A549 tumor-bearing mice were treated with PS432 i.p. at 2.5 mg/kg/day for 14 consecutive days. (A) Body weight changes of PS432-treated and control animals throughout the study duration. Data are presented as mean ± SEM. (B) Relative organ weight of PS432-treated and control animals at the end of the experiment. Horizontal and vertical lines indicate mean and SD, respectively.

SI Figure 9

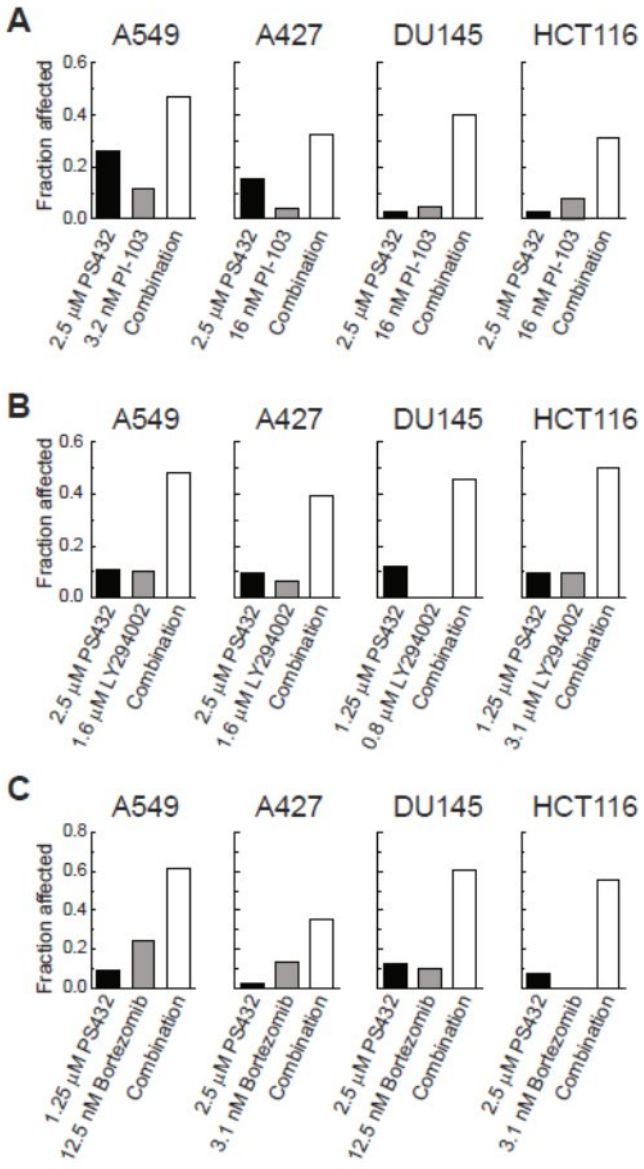

PS432 in combination with proteosome and PI3K inhibitors in different cancer cell lines. Screening identified that proteosome inhibitor bortezomib and PI3K inhibitors PI-103 and LY294002 have additive and synergistic effects in combination with PS432. (A) Graphs represent the fraction affected by PS432, PI-103 and their combination in lung (A549 and A427), prostate (DU145) and colon (HCT116) cancer cell lines. (B) and (C) Same as A but using LY294002 and bortezomib, respectively, in combination with PS432. An additive or synergistic effect between PS432 and PI-103 or LY294002 was confirmed in follow-up experiments. The effect of the combination of PS432 with the more clinically relevant PI3-kinase inhibitor BKM120

is presented in Figure 6. It may call the attention that PS432 has similar or higher potency in cells than in the above described *in vitro* effect on the activity of aPKCs. We suggest that selectivity assays that employ protein kinases stabilized in active conformations, as required for activity assays, may not measure the effect of compounds on the kinase in the cellular environment where the conformations are dynamically controlled by post-translational modifications and interacting proteins. The allosteric inhibitor compound PD098059 represents such example, since it potently inhibits the activation of MEK-1 but has much decreased ability to inhibit the activated form because it preferentially binds to an inactive conformation of the kinase (*28, 29*). In a similar manner, we expect that compounds that bind to inactive conformations of protein kinases may not show inhibitory effects in in vitro kinase assays but may be efficient kinase inhibitors in cells, thereby misleading on their presumed selectivity.

Supplemental References

1. Kabsch, W. (1993) Automatic Processing of Rotation Diffraction Data from Crystals of Initially Unknown Symmetry and Cell Constants, *Journal of Applied Crystallography 26*, 795-800.
2. Hindie, V., Stroba, A., Zhang, H., Lopez-Garcia, L. A., Idrissova, L., Zeuzem, S., Hirschberg, D., Schaeffer, F., Jorgensen, T. J. D., Engel, M., Alzari, P. M., and Biondi, R. M. (2009) Structure and allosteric effects of low molecular weight activators on the protein kinase PDK1, *Nat. Chem. Biol. 5*, 758-764.
3. McCoy, A. J., Grosse-Kunstleve, R. W., Adams, P. D., Winn, M. D., Storoni, L. C., and Read, R. J. (2007) Phaser crystallographic software, *J Appl Crystallogr 40*, 658-674.
4. Adams, P. D., Afonine, P. V., Bunkoczi, G., Chen, V. B., Davis, I. W., Echols, N., Headd, J. J., Hung, L. W., Kapral, G. J., Grosse-Kunstleve, R. W., McCoy, A. J., Moriarty, N. W., Oeffner, R., Read, R. J., Richardson, D. C., Richardson, J. S., Terwilliger, T. C., and Zwart, P. H. (2010) PHENIX: a comprehensive Python-based system for macromolecular structure solution, *Acta Crystallogr D Biol Crystallogr 66*, 213-221.
5. Emsley, P., and Cowtan, K. (2004) Coot: model-building tools for molecular graphics, *Acta Crystallogr D Biol Crystallogr 60*, 2126-2132.
6. DeLano (2002) *The PyMol User´s Manual*.
7. Pastor-Flores, D., Schulze, J. O., Bahi, A., Giacometti, R., Ferrer-Dalmau, J., Passeron, S., Engel, M., Suss, E., Casamayor, A., and Biondi, R. M. (2013) PIF-Pocket as a Target for C. albicans Pkh Selective Inhibitors, *Acs Chem Biol 8*, 2283-2292.
8. Chou, T. C. (2006) Theoretical basis, experimental design, and computerized simulation of synergism and antagonism in drug combination studies, *Pharmacol Rev 58*, 621-681.
9. Ke, N., Albers, A., Claassen, G., Yu, D. H., Chatterton, J. E., Hu, X., Meyhack, B., Wong-Staal, F., and Li, Q. X. (2004) One-week 96-well soft agar growth assay for cancer target validation, *Biotechniques 36*, 826-828, 830, 832-823.
10. Simon, R., Lam, A., Li, M. C., Ngan, M., Menenzes, S., and Zhao, Y. (2007) Analysis of gene expression data using BRB-ArrayTools, *Cancer Inform 3*, 11-17.
11. Reimand, J., Arak, T., and Vilo, J. (2011) g:Profiler--a web server for functional interpretation of gene lists (2011 update), *Nucleic Acids Res 39*, W307-315.
12. Subramanian, A., Tamayo, P., Mootha, V. K., Mukherjee, S., Ebert, B. L., Gillette, M. A., Paulovich, A., Pomeroy, S. L., Golub, T. R., Lander, E. S., and Mesirov, J. P. (2005) Gene set enrichment

analysis: a knowledge-based approach for interpreting genome-wide expression profiles, *Proc Natl Acad Sci U S A 102*, 15545-15550.
13. Oellerich, T., Bremes, V., Neumann, K., Bohnenberger, H., Dittmann, K., Hsiao, H. H., Engelke, M., Schnyder, T., Batista, F. D., Urlaub, H., and Wienands, J. (2011) The B-cell antigen receptor signals through a preformed transducer module of SLP65 and CIN85, *EMBO J 30*, 3620-3634.
14. Emsley, P., Lohkamp, B., Scott, W. G., and Cowtan, K. (2010) Features and development of Coot, *Acta Crystallogr D Biol Crystallogr 66*, 486-501.
15. Engel, M., Hindie, V., Lopez-Garcia, L. A., Stroba, A., Schaeffer, F., Adrian, I., Imig, J., Idrissova, L., Nastainczyk, W., Zeuzem, S., Alzari, P. M., Hartmann, R. W., Piiper, A., and Biondi, R. M. (2006) Allosteric activation of the protein kinase PDK1 with low molecular weight compounds, *Embo J 25*, 5469-5480.
16. Frodin, M., Antal, T. L., Dummler, B. A., Jensen, C. J., Deak, M., Gammeltoft, S., and Biondi, R. M. (2002) A phosphoserine/threonine-binding pocket in AGC kinases and PDK1 mediates activation by hydrophobic motif phosphorylation, *Embo J 21*, 5396-5407.
17. Zheng, J., Knighton, D. R., ten Eyck, L. F., Karlsson, R., Xuong, N., Taylor, S. S., and Sowadski, J. M. (1993) Crystal structure of the catalytic subunit of cAMP-dependent protein kinase complexed with MgATP and peptide inhibitor, *Biochemistry 32*, 2154-2161.
18. Biondi, R. M., Cheung, P. C., Casamayor, A., Deak, M., Currie, R. A., and Alessi, D. R. (2000) Identification of a pocket in the PDK1 kinase domain that interacts with PIF and the C-terminal residues of PKA, *Embo J 19*, 979-988.
19. Biondi, R. M., Komander, D., Thomas, C. C., Lizcano, J. M., Deak, M., Alessi, D. R., and van Aalten, D. M. (2002) High resolution crystal structure of the human PDK1 catalytic domain defines the regulatory phosphopeptide docking site, *Embo J 21*, 4219-4228.
20. Busschots, K., Lopez-Garcia, L. A., Lammi, C., Stroba, A., Zeuzem, S., Piiper, A., Alzari, P. M., Neimanis, S., Arencibia, J. M., Engel, M., Schulze, J. O., and Biondi, R. M. (2012) Substrate-Selective Inhibition of Protein Kinase PDK1 by Small Compounds that Bind to the PIF-Pocket Allosteric Docking Site, *Chem Biol 19*, 1152-1163.
21. Schulze, J. O., Saladino, G., Busschots, K., Neimanis, S., Suss, E., Odadzic, D., Zeuzem, S., Hindie, V., Herbrand, A. K., Lisa, M. N., Alzari, P. M., Gervasio, F. L., and Biondi, R. M. (2016) Bidirectional Allosteric Communication between the ATP-Binding Site and the Regulatory PIF Pocket in PDK1 Protein Kinase, *Cell Chem Biol 23*, 1193-1205.
22. Dettori, R., Sonzogni, S., Meyer, L., Lopez-Garcia, L. A., Morrice, N. A., Zeuzem, S., Engel, M., Piiper, A., Neimanis, S., Frodin, M., and Biondi, R. M. (2009) Regulation of the interaction between protein kinase C-related protein kinase 2 (PRK2) and its upstream kinase, 3-phosphoinositide-dependent protein kinase 1 (PDK1), *J Biol Chem 284*, 30318-30327.
23. Bauer, A. F., Sonzogni, S., Meyer, L., Zeuzem, S., Piiper, A., Biondi, R. M., and Neimanis, S. (2012) Regulation of protein kinase C-related protein kinase 2 (PRK2) by an intermolecular PRK2-PRK2 interaction mediated by its N-terminal domain, *J Biol Chem 287*, 20590-20602.
24. Lopez-Garcia, L. A., Schulze, J. O., Frohner, W., Zhang, H., Suss, E., Weber, N., Navratil, J., Amon, S., Hindie, V., Zeuzem, S., Jorgensen, T. J. D., Alzari, P. M., Neimanis, S., Engel, M., and Biondi, R. M. (2011) Allosteric Regulation of Protein Kinase PKC zeta by the N-Terminal C1 Domain and Small Compounds to the PIF-Pocket, *Chem Biol 18*, 1463-1473.
25. Zhang, H., Neimanis, S., Lopez-Garcia, L. A., Arencibia, J. M., Amon, S., Stroba, A., Zeuzem, S., Proschak, E., Stark, H., Bauer, A. F., Busschots, K., Jorgensen, T. J. D., Engel, M., Schulze, J. O., and Biondi, R. M. (2014) Molecular Mechanism of Regulation of the Atypical Protein Kinase C by N-terminal Domains and an Allosteric Small Compound, *Chem Biol 21*, 754-765.
26. Erdogan, E., Klee, E. W., Thompson, E. A., and Fields, A. P. (2009) Meta-analysis of oncogenic protein kinase Ciota signaling in lung adenocarcinoma, *Clin Cancer Res 15*, 1527-1533.

27. Rocha, A. S., Paternot, S., Coulonval, K., Dumont, J. E., Soares, P., and Roger, P. P. (2008) Cyclic AMP inhibits the proliferation of thyroid carcinoma cell lines through regulation of CDK4 phosphorylation, *Mol Biol Cell 19*, 4814-4825.
28. Alessi, D. R., Cuenda, A., Cohen, P., Dudley, D. T., and Saltiel, A. R. (1995) PD 098059 is a specific inhibitor of the activation of mitogen-activated protein kinase kinase in vitro and in vivo, *J Biol Chem 270*, 27489-27494.
29. Dudley, D. T., Pang, L., Decker, S. J., Bridges, A. J., and Saltiel, A. R. (1995) A synthetic inhibitor of the mitogen-activated protein kinase cascade, *Proc Natl Acad Sci U S A 92*, 7686-7689.